

Glow discharge growth of SnO<sub>2</sub> nano-needles from SnH<sub>4</sub><sup>†</sup>

Chun-Fang Wang, Su-Yuan Xie,\* Shui-Chao Lin, Xuan Cheng, Xian-Hua Zhang, Rong-Bin Huang\* and Lan-Sun Zheng

State Key Laboratory for Physical Chemistry of Solid Surfaces &amp; Department of Chemistry, Xiamen University, Xiamen, 361005, China. E-mail: syxie@jingxian.xmu.edu.cn; rbhuang@xmu.edu.cn

Received (in Cambridge, UK) 23rd March 2004, Accepted 26th May 2004

First published as an Advance Article on the web 29th June 2004

Single crystalline SnO<sub>2</sub> nano-needles with length up to 6–7 μm and diameter less than 300 nm are synthesized on an Au-coating porous silicon substrate from SnH<sub>4</sub> source via a glow discharge process.

SnO<sub>2</sub>, an n-type semiconductor with a wide band gap ( $E_g = 3.6$  eV, at 300 K), has been intensively investigated for its promising applications in optoelectronic devices,<sup>1</sup> gas sensors,<sup>2</sup> dye-based solar cells,<sup>2</sup> etc. To meet the contemporary requirement of instruments miniaturization, some one-dimensional (1D) nano-materials of SnO<sub>2</sub>, including rods,<sup>3</sup> wires,<sup>4–7</sup> tubes,<sup>7</sup> and belts or ribbons<sup>7–9</sup> have been fabricated by a number of physical and chemical processes. The constant lateral size in the 1D nano-material previously reported, however, may be problematic for application in some optoelectronic devices or sensors, e.g. as tips of scanning probes, field emitters, nanosensors or nanoindenters. Such shortcomings have recently stimulated synthetic interesting of pin-shaped nano-materials, e.g., conical carbon nanotubes<sup>10–12</sup> and ZnO nanoneedle.<sup>13,14</sup> Partly due to the synthetic difficulties, conical-shaped SnO<sub>2</sub> documented in literature is still scarce. Here we design a glow discharge method to synthesize SnO<sub>2</sub> nano-needles on an Au-coating porous silicon substrate, through feeding a decreasing SnH<sub>4</sub> source from the reaction between SnCl<sub>4</sub> and KBH<sub>4</sub>.

The experiment was performed in a combined setup that includes a SnH<sub>4</sub> generator (i.e., a three-necked flask) and a glow discharge system (see ESI<sup>†</sup>). 0.4 g SnCl<sub>4</sub>·5H<sub>2</sub>O was dissolved in 10 ml water, and then poured into the three-necked flask, which was equipped with a trickle filler containing 20 ml mixture solution of 0.010 g ml<sup>-1</sup> KBH<sub>4</sub> and 0.010 g ml<sup>-1</sup> KOH. When the basic solution of KBH<sub>4</sub> was added dropwise at a rate of 4 ml min<sup>-1</sup> into the SnCl<sub>4</sub> aqueous solution in the three-necked flask, SnH<sub>4</sub> gas was produced, and in turn, carried by O<sub>2</sub> at a flow of 10 ml min<sup>-1</sup> through a vent hole into the glow discharge chamber, which was a quartz tube placed in a horizontal tube furnace at a temperature of 800 °C. A pair of copper pipes, acting both as electrodes and gas passageway, were put at the two ends of the quartz tube. When the pressure of the reaction system was exhausted to less than 0.004 MPa and an alternating voltage of above 10 kV with 25 kHz frequency was applied to the electrodes, a stable glow discharge plasma would emerge at the gap between the two electrodes. The Au-coating porous silicon substrate was placed under the discharge plasma zone for SnO<sub>2</sub> deposition.

Fig. 1 shows the field-emission scanning electron microscopy (FE-SEM) images of the products taken on a LEO1530 SEM instrument. Nano-needles with length up to 6–7 μm, diameter less than 300 nm and conical angles of about 5–6°, accompanied by 35% (count from a 20 × 26 μm deposition zone) of nano-rods with lateral size of ~ 300 nm and 10% particles, were grown in the glow discharge process. From the zoom FE-SEM picture of the nano-needles/rods, some of them appear to be hexagonal pyramids with rough surfaces that seem to be constructed of a layer-by-layer structure. Both transmission electron microscopy (TEM) images taken by two kinds of TEM instruments, Fig. 2a and 2b, however,

show that there is no visible crack between the pseudo layers of the selected nano-needle with [100] axis growth direction. High-resolution TEM (HRTEM) picture (Fig. 2c) verifies that the nano-needle bears crystalline structure without any dislocation, which is supported by sharp diffraction peaks in corresponding X-ray powder diffraction (XRD) pattern recorded on a Rigaku DMAX/RC X-ray diffractometer using Cu-Kα radiation. As shown in Fig. 3, the diffraction peaks can be perfectly indexed to the tetragonal rutile structure of SnO<sub>2</sub> (JCPDS 41–1445), though there are some weak peaks arising from background impurity (e.g., silicon substrate produces a marked (111) peak at  $2\theta = 29.5^\circ$ ). The strong intensities of the SnO<sub>2</sub> diffraction peaks relative to the background signal indicates that the product has high purity of the SnO<sub>2</sub> rutile phase. The Raman spectrum (see ESI<sup>†</sup>), recorded using a confocal

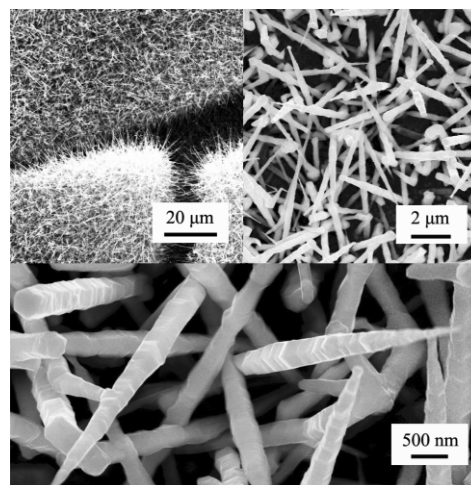


Fig. 1 FE-SEM images of the products with different zoom multiples.

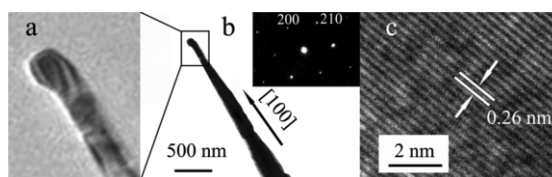


Fig. 2 TEM images from a selected SnO<sub>2</sub> nano-needle. (a) The tip recorded in a TECNAI F-30 FEG TEM instrument; (b) The nano-needle recorded in a JEM-100CXII instrument (with the inset of a selected area electron diffraction pattern); (c) HRTEM image with 0.26 nm distance corresponding to (101) of rutile SnO<sub>2</sub>.

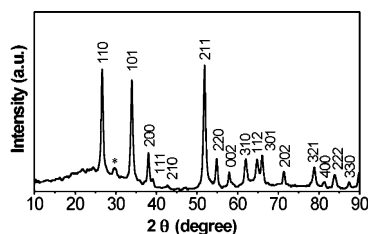


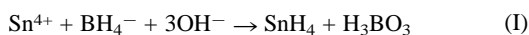
Fig. 3 X-Ray diffraction pattern of the products (\* the peak at  $2\theta = 29.5^\circ$  originates from the silicon substrate).

<sup>†</sup> Electronic supplementary information (ESI) available: diagram of the experimental setup used; Raman spectrum of the products. See <http://www.rsc.org/suppdata/cc/b4/b404362f>

microprobe Raman system (LabRam I from Dilor Inc. France) at excitation line of 632.8 nm, provides further evidence that the SnO<sub>2</sub> nano-needles adopt tetragonal rutile structure. The Raman shift peaks around 477.0, 635.6 and 774.6 cm<sup>-1</sup> with broadened widths are assigned to the E<sub>g</sub>, A<sub>1g</sub>, and B<sub>2g</sub> vibration modes, respectively.<sup>15</sup> Note that there is an additional peak at 522.0 cm<sup>-1</sup>, which appears to be sharper than the other three SnO<sub>2</sub> peaks and must come from the silicon substrate.

As shown in both FE-SEM and TEM images of the products, Fig. 1 and 2, polygonal or spherical particles are often observed at the tips of the SnO<sub>2</sub> nano-needles, which provides evidence that growth of the nano-conical SnO<sub>2</sub> is governed by the well-known vapor-liquid-solid (VLS) mechanism.<sup>16</sup> In a typical VLS process a nucleation catalyst is necessary for 1D material growth, and the diameter of the produced 1D material is directly related to the catalyst size. Our preliminary experiment confirms that the Au-coating on the silicon surface is key for the SnO<sub>2</sub> nuclei formation in the nanometer scale, but the possibility of the Au particles as the catalyst is ruled out because their sizes are apparently different from the as-produced nano-needles (Fig. 4a). The changing diameter of the nano-needle implies that catalyst size linked to the product diameter must be decreasing during the VLS growth process. We thus conjecture a self-catalytic VLS mechanism<sup>4</sup> involving decreasing size of Sn droplet catalyst to control the nano-needle growth, which is supported by the intermediates trapped from the reaction quenched through stopping the electronic supplies (for both glow discharge and furnace) and gas sources (of both O<sub>2</sub> and SnH<sub>4</sub>) more early than proposed process under otherwise the same reaction conditions. The total reaction times for the initial products shown in Fig. 4b and 4c are 0.5 min. and 1.5 min., respectively.

The reactions for SnO<sub>2</sub> nano-needles growth can be roughly described by the following equations:<sup>17,18</sup>



Reaction (I) provides the SnH<sub>4</sub> source and is performed in solution under mild conditions.<sup>17</sup> SnH<sub>4</sub> is known to decompose slowly at moderate temperatures but rapidly on a tin surface, while a small amount of oxygen can serve as protection gas to stop the decomposition due to the formation of an oxide film on the tin surface.<sup>18,19</sup> In the present experiment the glow-discharge provides an additional energy for SnH<sub>4</sub> decomposition. The nascent Sn from reaction (II) is deposited as liquid droplets on the surface of Au-coated silicon substrate to provide energetically favored sites for adsorption of oxygen.<sup>18,20</sup> SnO<sub>2</sub> is thus increasingly formed on the Sn droplet surface *via* reaction (III). At 800 °C, the SnO<sub>2</sub> layer on the surface is too mobile to seal the Sn liquid core, and subsequently dissolves into the Sn liquid to form an alloy droplet. Fig. 4b shows the alloy droplet quenched as nano-particle clusters with Sn and SnO<sub>2</sub> phases that exhibit different degrees of brightness in the

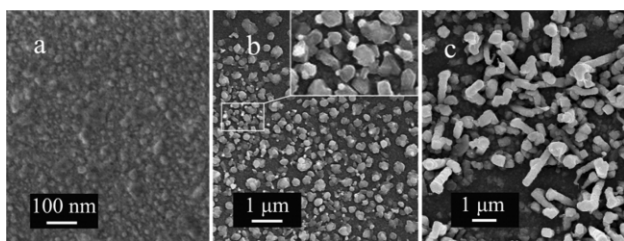


**Fig. 4** The FE-SEM images of (a) Au-coating porous silicon substrate; (b) Sn-SnO<sub>2</sub> alloy particles quenched; (c) SnO<sub>2</sub> nano-rod intermediates trapped in the glow discharge process.

enlarged SEM image (the inset to Fig. 4b). Energy-dispersive X-ray spectrometry also supported their Sn and SnO<sub>2</sub> composition. The continuous dissolution of SnO<sub>2</sub> leads to a supersaturated solution, which provides the driving force for 1D nano-materials growth (through precipitation of SnO<sub>2</sub> from the supersaturated droplets). Fig. 4c shows the middle stage of the SnO<sub>2</sub> solids trapped in the VLS process. Possibly due to the rapid anneal for quenching the reaction, the surface of the captured nano-rods appear to be rougher than the as-obtained SnO<sub>2</sub> nano-needles. In principle, the size of Sn catalyst and growth of the SnO<sub>2</sub> 1D material relies on the amount of SnH<sub>4</sub> fed, which is produced in SnH<sub>4</sub> generator and controlled by the addition rate of KBH<sub>4</sub>. In the present experiment, KBH<sub>4</sub> solution is added dropwise into the SnCl<sub>4</sub> solution at a constant rate of 4 ml min.<sup>-1</sup>. At the very beginning of the experiment, the concentration of SnCl<sub>4</sub> is high enough to produce a constant SnH<sub>4</sub> flow. With progress of reaction (I), however, SnH<sub>4</sub> flow would decrease in response to the consumption of SnCl<sub>4</sub> in the system. The changing SnH<sub>4</sub> flow would result in a decrease in size of the Sn catalyst, and subsequently would lead to formation of needle-shaped material. Moreover, adding KBH<sub>4</sub> into SnCl<sub>4</sub> solution in the drop-by-drop mode makes the SnH<sub>4</sub> flow in a discontinuous fashion, which, in turn, results in nano-needles with pseudo layer-by-layer structure as shown in Fig. 1.

In conclusion, the proposed glow discharge process has been successfully applied to synthesis of single crystalline SnO<sub>2</sub> nano-needles and a self-catalytic VLS mechanism is suggested to understand the conical materials growth. This method may be also extended to synthesize other semiconductive nano-needles materials by simply replacing SnH<sub>4</sub> with other hydrides, *e.g.*, GeH<sub>4</sub> and SiH<sub>4</sub>.

This work was supported by NNSF (Grant No. 20371041 and 20273052) and the Ministry of Science and Technology (2002CCA01600) and the Ministry of Education of China (03096). We would like to thank Dr. Wei Wang for his valuable discussion and generous help.

## Notes and references

- 1 A. Aoki and H. Sasakura, *Jpn. J. Appl. Phys.*, 1970, **9**, 582.
- 2 S. Ferrere, A. Zaban and B. A. Gsegg, *J. Phys. Chem. B*, 1997, **101**, 4490.
- 3 Y. K. Liu, C. L. Zheng, W. Z. Wang, C. R. Yin and G. H. Wang, *Adv. Mater.*, 2001, **13**, 1883.
- 4 Y. Q. Chen, X. F. Cui, K. Zhang, D. Y. Pan, S. Y. Zhang, B. Wang and J. G. Hou, *Chem. Phys. Lett.*, 2003, **369**, 16.
- 5 R. Q. Zhang, Y. Lifshitz and S. T. Li, *Adv. Mater.*, 2003, **15**, 635.
- 6 Y. L. Wang, X. C. Jiang and Y. N. Xia, *J. Am. Chem. Soc.*, 2003, **125**, 16176.
- 7 Z. R. Dai, J. L. Gole, J. D. Stout and Z. L. Wang, *J. Phys. Chem. B*, 2002, **106**, 1274.
- 8 Z. W. Pan, Z. R. Dai and Z. L. Wang, *Science*, 2001, **291**, 1947.
- 9 J. Q. Hu, X. L. Ma, N. G. Shang, Z. Y. Xie, N. B. Wong, C. S. Lee and S. T. Lee, *J. Phys. Chem. B*, 2002, **106**, 3823.
- 10 N. Muradov and A. Schwitter, *Nano Lett.*, 2002, **2**, 673.
- 11 G. Y. Zhang, X. Jiang and E. G. Wang, *Science*, 2003, **300**, 472.
- 12 R. C. Mani, X. Li, M. K. Sunkara and K. Rajan, *Nano Lett.*, 2003, **5**, 671.
- 13 J. Zhong, S. Muthukumar, Y. Chen, Y. Lu, H. M. Ng, W. Jiang and E. L. Garfunkel, *Appl. Phys. Lett.*, 2003, **83**, 3041.
- 14 Y. W. Zhu, H. Z. Zhang, X. C. Sun, S. Q. Feng, J. Xu, Q. Zhao, B. Xiang, R. M. Wang and D. P. Yu, *Appl. Phys. Lett.*, 2003, **83**, 144.
- 15 K. N. Yu, Y. H. Xiong, Y. L. Liu and C. S. Xiong, *Phys. Rev. B*, 1997, **55**, 2666.
- 16 R. S. Wagner and W. C. Ellis, *Appl. Phys. Lett.*, 1964, **4**, 89.
- 17 *Inorganic Syntheses Vol. VII*, ed. J. Kleinberg, McGraw-Hill, New York, 1963, p. 39.
- 18 K. Tamaru, *J. Phys. Chem.*, 1956, **60**, 610.
- 19 H. J. Emeléus and S. F. A. Kettle, *J. Chem. Soc.*, 1958, 2444.
- 20 *Constitution of Binary Alloys*, M. Hansen and K. Anderko, McGraw-Hill Book Company Inc., New York, 1958.